The $R_{D^{(*)}}$ and $R_{J/\psi}$ puzzles

Thang C. Tran

Università di Napoli Federico II & INFN – Napoli

(in collaboration with M.A. Ivanov, J.G. Körner, P. Santorelli)

[Phys.Rev. D92 (2015), 114022; Phys.Rev. D94 (2016), 094028; Phys.Rev. D95 (2017), 036021; Phys.Part.Nucl.Lett. 14 (2017), 669-676; Phys.Rev. D97 (2018), 054014]

Helmholtz-DIAS International Summer School
"QFT at the Limits: from Strong Fields to Heavy Quarks"
JINR, Dubna, July 22 – August 2, 2019

Outline

- **Introduction to semileptonic B decay: How to calculate the decay width in the SM + Helicity Amplitude technique**
- **Form factor in the Covariant Confining Quark Model**
- **Analyze possible NP effects in the decays $\bar{B}^0 \to D^{(*)}\tau^-\bar{\nu}_\tau$: general effective Hamiltonian approach + experimental constraints + observables**
- **More observables: Tau polarization and NP**
- **Implication of NP in $B_c \to (J/\psi, \eta_c)\tau\nu$**

Several *B*-decay diagrams

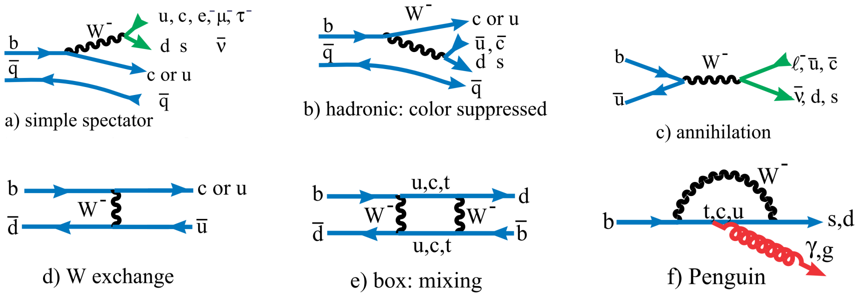

Figure: M. Artuso, E. Barberio, S. Stone, PMC Phys. A3 (2009) 3

Lectures in this School by P. Colangelo and D. Melikhov

Nonleptonic decays: Simplified VS. Realistic

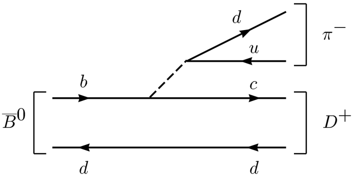

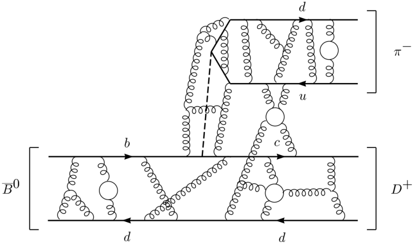

Figure: M. Neubert, hep-ph/0001334

Lectures in this School by P. Santorelli and M. A. Ivanov

(Purely) leptonic decays: Helicity suppressed & less rich phenomenology

$$\langle 0|\bar{q}\gamma^{\mu}\gamma_5 b|B(p_1)\rangle = -f_B p_1^{\mu}$$

$$\mathcal{B}(B^- \to \ell^- \bar{\nu}_\ell) = \frac{G_F^2}{8\pi}|V_{ub}|^2 \tau_B m_B m_\ell^2 \left(1 - \frac{m_\ell^2}{m_B^2}\right)^2 f_B^2,$$

$\approx O(10^{-4})$, $O(10^{-7})$, and $O(10^{-11})$ for $\ell = \tau, \mu, e$

- $B \to D^{(*)}\ell\bar{\nu}_\ell$ proceed via two sub-processes $b \to cW^{*-}$ and $W^{*-} \to \ell\bar{\nu}_\ell$
- Lepton pair is invisible to the strong force
- Matrix element in SM

$$\mathcal{M}(B \to D^{(*)}\ell\bar{\nu}_\ell) = \frac{G_F}{\sqrt{2}} V_{cb} H^\mu L_\mu,$$

- leptonic and hadronic matrix elements

$$\begin{aligned} L_\mu &= \bar{\ell}\gamma_\mu(1-\gamma_5)\nu_\ell, \\ H^\mu &= \left\langle D^{(*)} \left| V^\mu - A^\mu \right| B \right\rangle, \end{aligned}$$

where $V^\mu = \bar{c}\gamma^\mu b$ and $A^\mu = \bar{c}\gamma^\mu\gamma_5 b$ are flavor-changing vector and axial-vector currents, respectively.

- H^μ is constructed from four-vectors appearing in the transition (4-momenta and polarization vectors).
- For $B(p_1) \to D(p_2)$ ($P = p_1 + p_2$, $q = p_1 - p_2$):

$$\langle D(p_2)|V^\mu|B(p_1)\rangle = F_+(q^2)P^\mu + F_-(q^2)q^\mu$$

- For $B(p_1) \to D^*(p_2, \epsilon_2)$

$$\begin{aligned}\langle D^*(p_2, \epsilon_2)|V^\mu - A^\mu|B(p_1)\rangle &= \frac{\epsilon^*_{2\alpha}}{M_1 + M_2}\Big[- g^{\mu\alpha} P \cdot q A_0(q^2) + P^\mu P^\alpha A_+(q^2) \\ &\quad + q^\mu P^\alpha A_-(q^2) + i\varepsilon^{\mu\alpha P q} V(q^2)\Big],\end{aligned}$$

- where ϵ_2 - polarization vector of D^* so that $\epsilon^*_2 \cdot p_2 = 0$
- The particles are on shell: $p_1^2 = m_1^2 = m_B^2$, $p_2^2 = m_2^2 = m^2_{D^{(*)}}$.
- V^μ contributes to the FF $V(q^2)$, while A^μ – to $A_{\pm,0}(q^2)$.

Decay distribution and Helicity basis

$$\frac{d\Gamma}{dq^2 d\cos\theta} = \frac{|\mathrm{p}_2|}{(2\pi)^3\, 32\, m_1^2}\left(1-\frac{m_\ell^2}{q^2}\right)\cdot\sum_{\mathrm{pol}}|M|^2 = \frac{G_F^2|V_{cb}|^2}{(2\pi)^3}\,\frac{|\mathrm{p}_2|}{64 m_1^2}\left(1-\frac{m_\ell^2}{q^2}\right) H^{\mu\nu} L_{\mu\nu}\,,$$

where $|\mathrm{p}_2| = \lambda^{1/2}(m_1^2, m_2^2, q^2)/2m_1$ – momentum of $D^{(*)}$ in B rest frame, and θ - polar angle between $\vec{q} = \vec{p}_1 - \vec{p}_2$ and $\vec{k}_1$ in $(\ell^- \bar{\nu}_\ell)$ rest frame.

$$\begin{aligned} L_{\mu\nu} &= \mathrm{tr}\left[(\not k_1 + m_\ell)\gamma_\mu(1-\gamma_5)\ \not k_2 \gamma_\nu (1-\gamma_5)\right] \\ &= 8\left(k_{1\mu}k_{2\nu} + k_{1\nu}k_{2\mu} - k_1 k_2 g_{\mu\nu} + i\varepsilon_{\mu\nu k_1 k_2}\right) \end{aligned}$$

$$\begin{aligned} H^{\mu\nu} &= \sum_{\mathrm{pol}} \langle D^{(*)}|V^\mu - A^\mu|B\rangle \cdot \langle D^{(*)}|V^\nu - A^\nu|B\rangle^\dagger \\ &= \begin{cases} H_\mu H_\nu^\dagger & \text{for} \quad B \to D \\ h_{\mu\alpha} h_{\nu\beta}^\dagger \left(-g^{\alpha\beta} + \frac{p_2^\alpha p_2^\beta}{M_2^2}\right) & \text{for} \quad B \to D^* \end{cases}, \end{aligned}$$

where $h_{\mu\alpha}$ is defined by: $H_\mu = \epsilon_2^{\dagger\alpha} h_{\mu\alpha}$.

- The Lorentz contraction can be evaluated in terms of the helicity amplitudes.
  J. G. Körner, G. A. Schuler, Z. Phys. C 38, 511 (1988), Phys. Lett. B 231, 306 (1989)
- Orthonormal and complete helicity basis $\epsilon^\mu(\lambda_W)$ with three spin-1 components orthogonal to the momentum transfer q^μ, i.e., $\epsilon^\mu(\lambda_W)q_\mu = 0$, for $\lambda_W = \pm, 0$, and one spin-0 (time) component $\lambda_W = t$ with $\epsilon^\mu(t) = q^\mu/\sqrt{q^2}$.

$$
\begin{aligned}
\epsilon^\dagger_\mu(m)\epsilon^\mu(n) &= g_{mn} \quad \text{(orthonormality)},\\
\epsilon_\mu(m)\epsilon^\dagger_\nu(n)g_{mn} &= g_{\mu\nu} \quad \text{(completeness)},
\end{aligned}
$$

with $m, n = \lambda_W = t, \pm, 0$ and $g_{mn} = \mathrm{diag}(+, -, -, -)$.
- Rewrite the contraction using the completeness relation

$$
\begin{aligned}
H^{\mu\nu}L_{\mu\nu} &= \sum_{m,m',n,n'} H(m,n)L(m',n')g_{mm'}g_{nn'}\,, \quad (m^{(\prime)}, n^{(\prime)} = \lambda_W = t, \pm, 0)\\
L(m,n) &= L^{\mu\nu}\epsilon_\mu(m)\epsilon^\dagger_\nu(n)\\
H(m,n) &= H^{\mu\nu}\epsilon^\dagger_\mu(m)\epsilon_\nu(n)
\end{aligned}
$$

- $L(m,n)$ and $H(m,n)$ *can now be evaluated in different Lorentz systems:* $L(m,n)$ - *in the* $(\ell^-\bar{\nu}_\ell)$*-CM system whereas* $H(m,n)$ - *in the B rest system.*

In the B rest frame, the momenta and polarization vectors $\epsilon^\mu(\lambda_W)$ can be written as

$$
\begin{aligned}
p_1^\mu &= (m_1, 0, 0, 0), & \epsilon^\mu(t) &= \frac{1}{\sqrt{q^2}}(q_0, 0, 0, |\mathbf{p}_2|), \\
p_2^\mu &= (E_2, 0, 0, -|\mathbf{p}_2|), & \epsilon^\mu(\pm) &= \frac{1}{\sqrt{2}}(0, \mp 1, -i, 0), \\
q^\mu &= (q_0, 0, 0, +|\mathbf{p}_2|), & \epsilon^\mu(0) &= \frac{1}{\sqrt{q^2}}(|\mathbf{p}_2|, 0, 0, q_0),
\end{aligned}
$$

where $E_2 = (m_1^2 + m_2^2 - q^2)/2m_1$ and $q_0 = (m_1^2 - m_2^2 + q^2)/2m_1$.

(a) $B \to D$: $\boxed{H_{\lambda_W} = \epsilon^{\dagger\mu}(\lambda_W) H_\mu}$

$$H(m, n) = \left(\epsilon^{\dagger\mu}(m) H_\mu\right) \cdot \left(\epsilon^{\dagger\nu}(n) H_\nu\right)^\dagger \equiv H_m H_n^\dagger.$$

$$H_t = \frac{1}{\sqrt{q^2}}[(m_1^2 - m_2^2) F_+(q^2) + q^2 F_-(q^2)], \quad H_0 = \frac{2m_1|\mathbf{p}_2|}{\sqrt{q^2}} F_+(q^2), \quad H_\pm = 0$$

Helicity Amplitudes

(b) $B \to D^*$: $\boxed{H_{\lambda_W \lambda_{D^*}} = \epsilon^{\dagger\mu}(\lambda_W)\epsilon_2^{\dagger\alpha}(\lambda_{D^*})h_{\mu\alpha}}$

$$
\begin{aligned}
H(m,n) &= \epsilon^{\dagger\mu}(m)\epsilon^{\nu}(n)H_{\mu\nu} = \epsilon^{\dagger\mu}(m)\epsilon^{\nu}(n)h_{\mu\alpha}\epsilon_2^{\dagger\alpha}(r)\epsilon_2^{\beta}(s)\delta_{rs}h^{\dagger}_{\beta\nu} \\
&= \epsilon^{\dagger\mu}(m)\epsilon_2^{\dagger\alpha}(r)h_{\mu\alpha}\cdot\left(\epsilon^{\dagger\nu}(n)\epsilon_2^{\dagger\beta}(s)h_{\nu\beta}\right)^{\dagger}\delta_{rs} \equiv H_{mr}H^{\dagger}_{nr}.
\end{aligned}
$$

In addition to the $W_{\rm offshell}$ polarization four-vectors $\epsilon^{\mu}(\lambda_W)$ one needs the polarization four-vectors $\epsilon_2^{\alpha}(\lambda_{D^*})$ of the D^*:

$$
\epsilon_2^{\alpha}(\pm) = \frac{1}{\sqrt{2}}(0\,,\ \pm 1\,,\ -i\,,\ 0\,)\,, \qquad \epsilon_2^{\alpha}(0) = \frac{1}{m_2}(|\mathbf{p}_2|\,,\ 0\,,\ 0\,,\ -E_2\,).
$$

$$
\begin{aligned}
H_t \equiv H_{t0} &= \frac{1}{m_1+m_2}\frac{m_1|\mathbf{p}_2|}{m_2\sqrt{q^2}}[(m_1^2-m_2^2)(A_+(q^2)-A_0(q^2))+q^2A_-(q^2)]\,, \\
H_{\pm} \equiv H_{\pm\pm} &= \frac{1}{m_1+m_2}[-(m_1^2-m_2^2)A_0(q^2)\pm 2m_1|\mathbf{p}_2|V(q^2)]\,, \\
H_0 \equiv H_{00} &= \frac{1}{m_1+m_2}\frac{1}{m_2\sqrt{q^2}}[(m_2^2-m_1^2)(m_1^2-m_2^2-q^2)A_0(q^2)+4m_1^2|\mathbf{p}_2|^2A_+(q^2)]
\end{aligned}
$$

Decay distribution in terms of Helicity amplitudes

$$\frac{d\Gamma(B\to D^{(*)}\ell^-\bar{\nu}_\ell)}{dq^2 d\cos\theta} = \frac{G_F^2|V_{cb}|^2|\mathbf{p}_2|q^2}{32(2\pi)^3 m_1^2}\left(1-\frac{m_\ell^2}{q^2}\right)^2 \times$$

$$\times \left\{(1-\cos\theta)^2|H_+|^2 + (1+\cos\theta)^2|H_-|^2 + 2\sin^2\theta|H_0|^2 + \frac{m_\ell^2}{q^2}\left[\sin^2\theta(|H_+|^2+|H_-|^2) + 2|H_t - H_0\cos\theta|^2\right]\right\}$$

$$\frac{d\Gamma(B\to D^{(*)}\ell^-\bar{\nu}_\ell)}{dq^2} = \frac{G_F^2|V_{cb}|^2|\mathbf{p}_2|q^2}{12(2\pi)^3 m_1^2}\left(1-\frac{m_\ell^2}{q^2}\right)^2 \times$$

$$\times \left\{(|H_+|^2+|H_-|^2+|H_0|^2)\left(1+\frac{m_\ell^2}{2q^2}\right) + \frac{3m_\ell^2}{2q^2}|H_t|^2\right\}$$

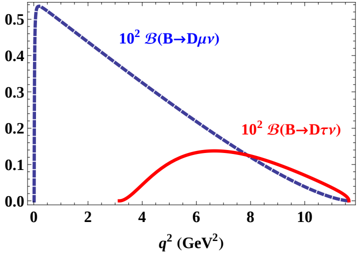

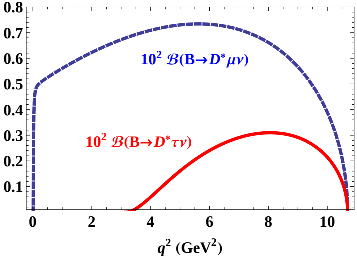

Form factors in the CCQM

G. V. Efimov, M. A. Ivanov, V. E. Lyubovitskij, J. G. Körner, P. Santorelli,. . .

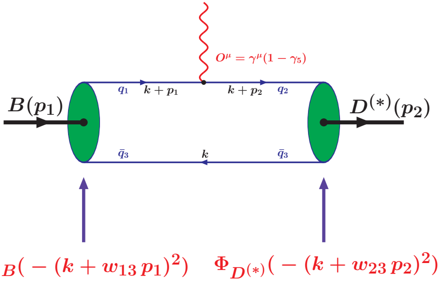

Matrix elements are described by a set of Feynman diagrams which are convolutions of quark propagators and vertex functions.

$$\langle D^*(p_2,\epsilon_2)\,|\,V^\mu - A^\mu\,|\,B(p_1)\rangle =$$

$$= \quad N_c\, g_B\, g_{D^*} \int \frac{d^4k}{(2\pi)^4 i}\, \widetilde{\Phi}_B\Big(-(k+w_{13}p_1)^2\Big)\, \widetilde{\Phi}_{D^*}\Big(-(k+w_{23}p_2)^2\Big)$$

$$\times \quad \mathrm{tr}\Big[\gamma^\mu(1-\gamma_5)\, S_1(k+p_1)\, \gamma^5\, S_3(k)\; \not{\epsilon}_2^{\,\dagger}\, S_2(k+p_2)\Big]$$

- Use the Fock-Schwinger representation of the quark propagator:

$$\begin{aligned} S_q(k+wp) &= \frac{1}{m_q - \not k - w \not p} = \frac{m_q + \not k + w \not p}{m_q^2 - (k+wp)^2} \\ &= (m_q + \not k + w \not p) \int\limits_0^\infty d\alpha \, e^{-\alpha[m_q^2 - (k+wp)^2]} \end{aligned}$$

- Nonlocal Gaussian-type vertex functions with fall-off behavior in Euclidean space to temper high energy divergence of quark loops

$$\widetilde{\Phi}_H(-k^2) = \int dx \, e^{ikx} \Phi_H(x^2) = e^{k^2/\Lambda_H^2}$$

where Λ_H characterizes the meson size.
- We imply that the loop integration k proceed over Euclidean space:

$$k^0 \to e^{i\frac{\pi}{2}} k_4 = ik_4 \,, \qquad k^2 = (k^0)^2 - \vec{k}^{\,2} \to -k_E^2 \leq 0 \,.$$

- We simultaneously rotate all external momenta, i.e. $p_0 \to ip_4$ so that $p^2 = -p_E^2 \leq 0$. Then the quadratic form in the exponent becomes positive-definite,

$$m_q^2 - (k+wp)^2 = m_q^2 + (k_E + wp_E)^2 > 0,$$

and the integral over α is absolutely convergent.

Quark-Meson coupling

- **Compositeness condition** $Z_H = 0$

Salam 1962; Weinberg 1963

Z_H – wave function renormalization constant of the meson H.

$$\boxed{Z_H^{1/2} = < H_{\rm bare} | H_{\rm dressed} > = 0}$$

- $Z_H = 1 - \tilde{\Pi}'(m_H^2) = 0$ where $\tilde{\Pi}(p^2)$ is the meson mass operator.

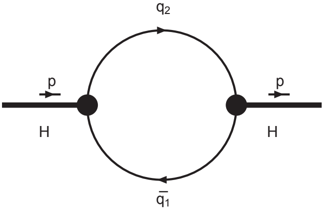

$$\Pi_P(p) = 3 g_P^2 \int \frac{dk}{(2\pi)^4 i} \widetilde{\Phi}_P^2(-k^2) \mathrm{tr}[S_1(k + w_1 p)\gamma^5 S_2(k - w_2 p)\gamma^5]$$

$$\Pi_V(p) = g_V^2 [g^{\mu\nu} - \frac{p^\mu p^\nu}{p^2}] \int \frac{dk}{(2\pi)^4 i} \widetilde{\Phi}_V^2(-k^2) \mathrm{tr}\,[S_1(k + w_1 p)\gamma_\mu S_2(k - w_2 p)\gamma_\nu]$$

Infrared confinement & Model parameters

One obtains $\Pi = \int\limits_0^\infty d^n\alpha\, F(\alpha_1,\ldots,\alpha_n),$

where F stands for the whole structure of a given diagram. The set of Schwinger parameters α_i can be turned into a simplex by introducing an additional t–integration via the identity $1 = \int\limits_0^\infty dt\, \delta(t - \sum\limits_{i=1}^n \alpha_i)$

$$\Pi = \int\limits_0^\infty dt t^{n-1} \int\limits_0^1 d^n\alpha\, \delta\Big(1 - \sum_{i=1}^n \alpha_i\Big)\, F(t\alpha_1,\ldots,t\alpha_n)\,.$$

Cut off the upper integration at $1/\lambda^2$

$$\boxed{\Pi^c = \int\limits_0^{1/\lambda^2} dt t^{n-1} \int\limits_0^1 d^n\alpha\, \delta\Big(1 - \sum_{i=1}^n \alpha_i\Big)\, F(t\alpha_1,\ldots,t\alpha_n)}$$

The infrared cut-off has removed all possible thresholds in the quark loop diagram.

MODEL PARAMETERS (all in GeV):

$m_{u/d}$	m_c	m_b	Λ_{D^*}	Λ_D	Λ_B	λ
0.241	1.67	5.04	1.53	1.60	1.96	0.181

Form factors

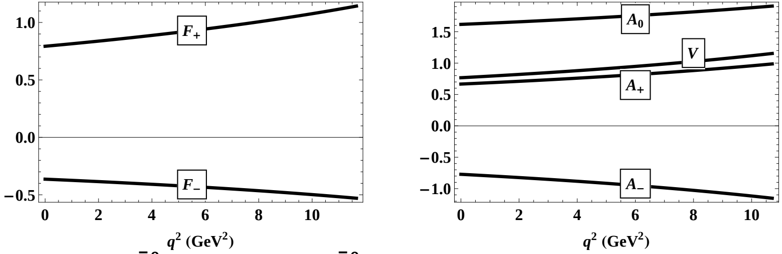

Form factors for $\bar{B}^0 \to D$ (left) and $\bar{B}^0 \to D^*$ (right) in the full momentum transfer range $0 \leq q^2 \leq q^2_{max} = (m_{\bar{B}^0} - m_{D^{(*)}})^2$.

- **Dipole interpolation**

$$F(q^2) = \frac{F(0)}{1 - as + bs^2}, \quad s = \frac{q^2}{m^2_{D^{(*)}}}.$$

- **The dipole interpolation works very well for all form factors:**
  dotted: calculated by FORTRAN
  solid: interpolation

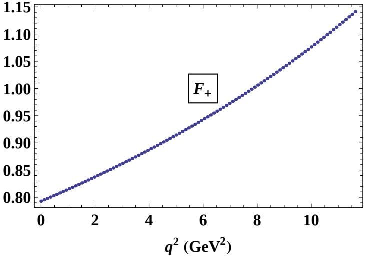

The parameters of the dipole interpolation $F(q^2) = \dfrac{F(0)}{1 - as + bs^2}$:

	F_+	F_-	A_0	A_+	A_-	V
$F(0)$	0.78	-0.36	1.62	0.67	-0.77	0.77
a	0.74	0.76	0.34	0.87	0.89	0.90
b	0.038	0.046	-0.16	0.057	0.070	0.075
$F(q^2_{\rm max})$	1.14	-0.53	1.91	0.99	-1.15	1.15
$F^{HQL}(q^2_{\rm max})$	1.14	-0.54	1.99	1.12	-1.12	1.12

The FF ratio exhibits linear q^2 behavior

D. Becirevic, N. Kosnik, A. Tayduganov, PLB 716, 208 (2012).

$$
\begin{aligned}
F_0(q^2) &= F_+(q^2) + \frac{q^2}{Pq} F_-(q^2) \\
\frac{F_0(q^2)}{F_+(q^2)} &= 1 - \alpha q^2,
\end{aligned}
$$

where the slope $\alpha = 0.020(1)\ \mathrm{GeV}^{-2}$ based on lattice results of the two FFs.

Our value: $\alpha = 0.019\ \mathrm{GeV}^{-2}$.

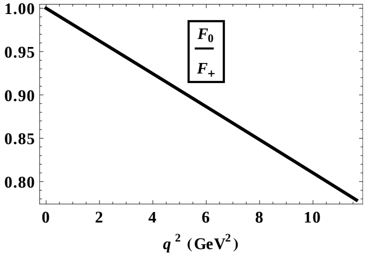

Motivation

- **Testing the Standard Model**
- **CKM matrix element $|V_{cb}|$**
- **Form factors of hadronic transitions**
- **Possible NP beyond the SM**

Ratios of branching fractions:

$$\boxed{R(D^{(*)}) \equiv \frac{\mathcal{B}(\bar{B}^0 \to D^{(*)}\tau^-\bar{\nu}_\tau)}{\mathcal{B}(\bar{B}^0 \to D^{(*)}\mu^-\bar{\nu}_\mu)}}$$

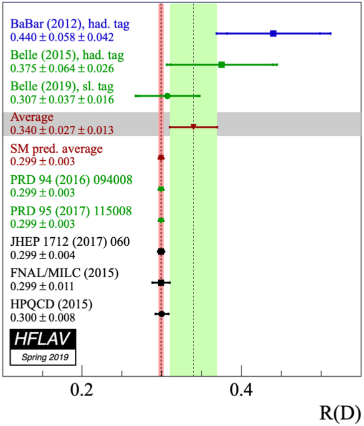

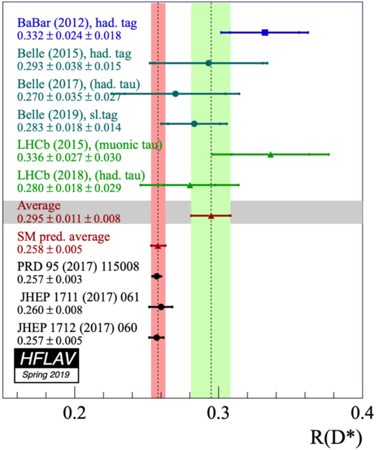

SM excess: 1.4σ and 2.5σ, respectively. (Before Belle-2019: 2.3σ and 3.0σ)

Motivation

$R(D)$-$R(D^*)$ combined: SM excess $\approx 3.1\sigma$ (Before Belle-2019: $\approx 3.8\sigma$)

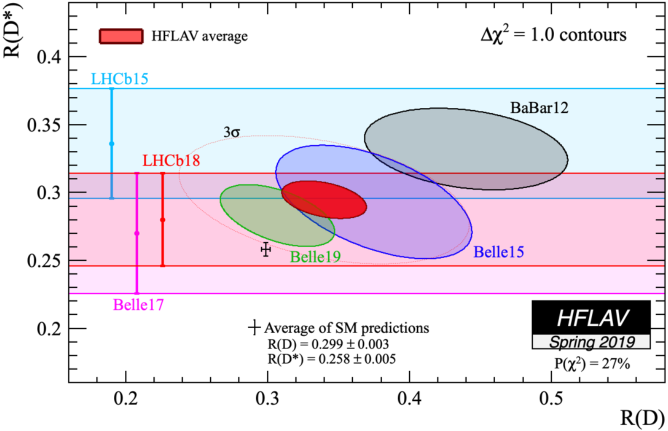

Theoretical attempts to explain the excess:

- **Specific NP models: two-Higgs-doublet models (2HDMs), Minimal Supersymmetric Standard Model (MSSM), Leptoquark models, etc.**
- **Impose general SM+NP effective Hamiltonian for transition $b \to c\ell\bar{\nu}$.**

Possible New Physics in the decays $B \to D^{(*)}\tau\nu_\tau$

Effective Hamiltonian for the quark-level transition $b \to c\tau^-\bar{\nu}_\tau$

$$\boxed{\mathcal{H}_{eff} = 2\sqrt{2}G_F V_{cb}[(1 + V_L)\mathcal{O}_{V_L} + V_R\mathcal{O}_{V_R} + S_L\mathcal{O}_{S_L} + S_R\mathcal{O}_{S_R} + T_L\mathcal{O}_{T_L}]}$$

where the four-fermion operators are written as

$$\begin{aligned}
\mathcal{O}_{V_L} &= (\bar{c}\gamma^\mu P_L b)\,(\bar{\tau}\gamma_\mu P_L \nu_\tau) \Leftarrow \text{SM Operator} \\
\mathcal{O}_{V_R} &= (\bar{c}\gamma^\mu P_R b)\,(\bar{\tau}\gamma_\mu P_L \nu_\tau) \\
\mathcal{O}_{S_L} &= (\bar{c}P_L b)\,(\bar{\tau}P_L \nu_\tau) \\
\mathcal{O}_{S_R} &= (\bar{c}P_R b)\,(\bar{\tau}P_L \nu_\tau) \\
\mathcal{O}_{T_L} &= (\bar{c}\sigma^{\mu\nu} P_L b)\,(\bar{\tau}\sigma_{\mu\nu} P_L \nu_\tau)
\end{aligned}$$

- **Here, $\sigma_{\mu\nu} = i\,[\gamma_\mu, \gamma_\nu]\,/2$**
- **$P_{L,R} = (1 \mp \gamma_5)/2$ - the left and right projection operators**
- **$V_{L,R}$, $S_{L,R}$, and T_L - complex Wilson coefficients governing NP contributions.**
- **In the SM: $V_{L,R} = S_{L,R} = T_L = 0$.**
- **Assumption: neutrino is always left handed and NP only affects leptons of the third generation.**

Lectures in this School by P. Colangelo and A. Grozin

Matrix element and NP form factors

$$\begin{aligned}\mathcal{M} &= \frac{G_F V_{cb}}{\sqrt{2}}\Big[(1+V_R+V_L)\langle D^{(*)}|\bar{c}\gamma^{\mu}b|\bar{B}^0\rangle\bar{\tau}\gamma_{\mu}(1-\gamma^5)\nu_{\tau}\\
&\quad+(V_R-V_L)\langle D^{(*)}|\bar{c}\gamma^{\mu}\gamma^5 b|\bar{B}^0\rangle\bar{\tau}\gamma_{\mu}(1-\gamma^5)\nu_{\tau}\\
&\quad+(S_R+S_L)\langle D^{(*)}|\bar{c}b|\bar{B}^0\rangle\bar{\tau}(1-\gamma^5)\nu_{\tau}\\
&\quad+(S_R-S_L)\langle D^{(*)}|\bar{c}\gamma^5 b|\bar{B}^0\rangle\bar{\tau}(1-\gamma^5)\nu_{\tau}\\
&\quad+T_L\langle D^{(*)}|\bar{c}\sigma^{\mu\nu}(1-\gamma^5)b|\bar{B}^0\rangle\bar{\tau}\sigma_{\mu\nu}(1-\gamma^5)\nu_{\tau}\Big].\end{aligned}$$

The axial and pseudoscalar hadronic matrix elements do not contribute to $\bar{B}^0\to D$; and the scalar hadronic matrix element does not contribute to $\bar{B}^0\to D^*$.

We need more form factors to describe NP operators:

$$\begin{aligned}\langle D(p_2)|\bar{c}b|\bar{B}^0(p_1)\rangle &= (m_1+m_2)F^S(q^2),\\
\langle D(p_2)|\bar{c}\sigma^{\mu\nu}(1-\gamma^5)b|\bar{B}^0(p_1)\rangle &= \frac{iF^T(q^2)}{m_1+m_2}\left(P^{\mu}q^{\nu}-P^{\nu}q^{\mu}+i\varepsilon^{\mu\nu Pq}\right),\end{aligned}$$

$$\begin{aligned}\langle D^*(p_2)|\bar{c}\gamma^5 b|\bar{B}^0(p_1)\rangle &= \epsilon^{\dagger}_{2\alpha}P^{\alpha}G^S(q^2),\\
\langle D^*(p_2)|\bar{c}\sigma^{\mu\nu}(1-\gamma^5)b|\bar{B}^0(p_1)\rangle &= -i\epsilon^{\dagger}_{2\alpha}\Big[\left(P^{\mu}g^{\nu\alpha}-P^{\nu}g^{\mu\alpha}+i\varepsilon^{P\mu\nu\alpha}\right)G_1^T(q^2)\\
&\quad+\left(q^{\mu}g^{\nu\alpha}-q^{\nu}g^{\mu\alpha}+i\varepsilon^{q\mu\nu\alpha}\right)G_2^T(q^2)\\
&\quad+\left(P^{\mu}q^{\nu}-P^{\nu}q^{\mu}+i\varepsilon^{Pq\mu\nu}\right)P^{\alpha}\frac{G_0^T(q^2)}{(m_1+m_2)^2}\Big],\end{aligned}$$

Form factors for NP operators

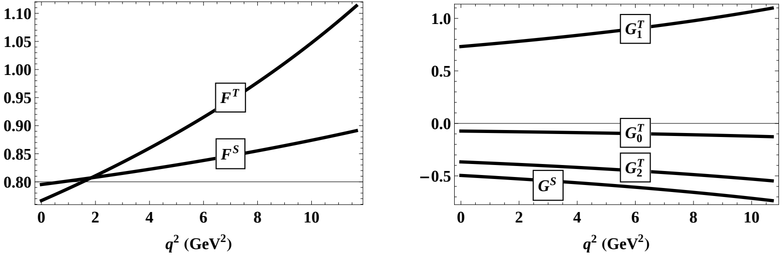

NP form factors for $\bar{B}^0 \to D$ (left) and $\bar{B}^0 \to D^*$ (right) in the full momentum transfer range $0 \leq q^2 \leq q^2_{max} = (m_{\bar{B}^0} - m_{D^{(*)}})^2$.

The parameters of the dipole interpolation:

	F^S	F^T	G^S	G_0^T	G_1^T	G_2^T
$F(0)$	0.80	0.77	−0.50	−0.073	0.73	−0.37
a	0.22	0.76	0.87	1.23	0.90	0.88
b	−0.098	0.043	0.060	0.33	0.074	0.064
$F(q^2_{\rm max})$	0.89	1.11	−0.73	−0.13	1.10	−0.55
$F^{HQL}(q^2_{\rm max})$	0.88	1.14	−0.62	0	1.12	−0.50

Form factors comparison

HQET form factors taken from a recent paper by Alonso-Kobach-Camalich [arXiv:1602.07671], **here** $F_0(q^2) = F_+(q^2) + \frac{q^2}{m_1^2 - m_2^2} F_-(q^2)$.

(Caprini-Lellouch-Neubert parametrization, except for $F_0(q^2)$**, where they used the Bourrely-Caprini-Lellouch parametrization)**

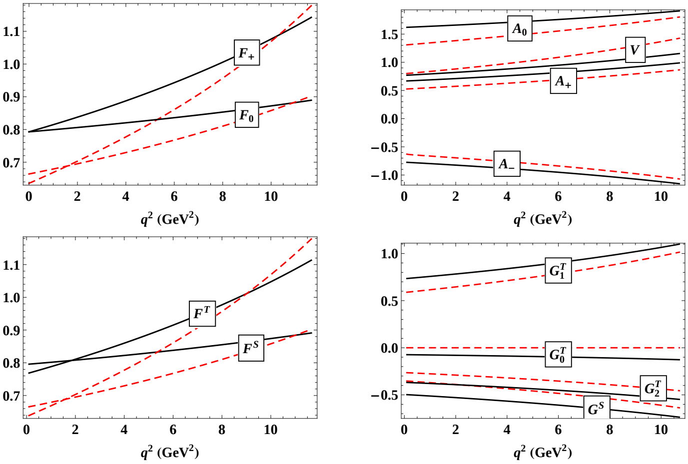

Ratios of branching fractions

$$R_{D^{(*)}}(q^2) = \left(\frac{q^2 - m_\tau^2}{q^2 - m_\mu^2}\right)^2 \frac{\mathcal{H}_{tot}^{D^{(*)}}}{\sum_n |H_n|^2 + \delta_\mu\left(\sum_n |H_n|^2 + 3|H_t|^2\right)},$$

where

$$\begin{aligned}
\mathcal{H}_{tot}^{D} &= |1+g_V|^2\left[|H_0|^2 + \delta_\tau(|H_0|^2 + 3|H_t|^2)\right] + \frac{3}{2}|g_S|^2|H_P^S|^2 \\
&\quad + 3\sqrt{2\delta_\tau}\,\mathrm{Re}\,g_S H_P^S H_t + 8|T_L|^2(1+4\delta_\tau)|H_T|^2 + 12\sqrt{2\delta_\tau}\,\mathrm{Re}\,T_L H_0 H_T,
\end{aligned}$$

$$\begin{aligned}
\mathcal{H}_{tot}^{D^*} &= (|1+V_L|^2 + |V_R|^2)\left[\sum_n |H_n|^2 + \delta_\tau\left(\sum_n |H_n|^2 + 3|H_t|^2\right)\right] + \frac{3}{2}|g_P|^2|H_V^S|^2 \\
&\quad - 2\,\mathrm{Re}\,V_R\left[(1+\delta_\tau)(|H_0|^2 + 2H_+H_-) + 3\delta_\tau|H_t|^2\right] - 3\sqrt{2\delta_\tau}\,\mathrm{Re}\,g_P H_V^S H_t \\
&\quad + 8|T_L|^2(1+4\delta_\tau)\sum_n |H_T^n|^2 - 12\sqrt{2\delta_\tau}\,\mathrm{Re}\,T_L \sum_n H_n H_T^n.
\end{aligned}$$

Here, $\delta_\ell = m_\ell^2/2q^2$, $g_V \equiv V_L + V_R$, $g_S \equiv S_L + S_R$, $g_P \equiv S_L - S_R$, and the index n runs through $(0, +, -)$.

Assuming that besides the SM contribution, only one of the NP operators is switched on at a time, and NP only affects the tau modes. (+10% theor. error)

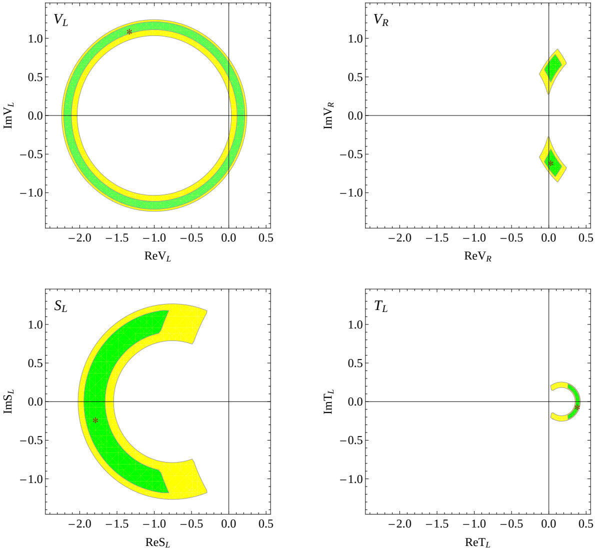

The allowed regions of the Wilson coefficients $V_{L,R}$, S_L, and T_L within 1σ (green, dark) and 2σ (yellow, light). The best-fit value in each case is denoted with the symbol $*$. The coefficient S_R is disfavored at 2σ and therefore is not shown here.

The $\bar{B}^0 \to D^{*+}(\to D^0\pi^+)\tau^-\bar{\nu}_\tau$ four-fold distribution

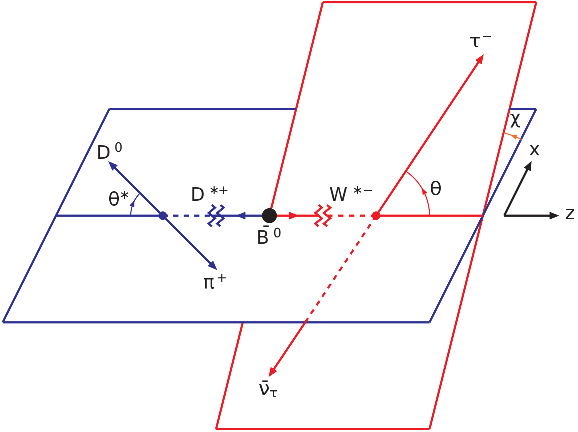

One has

$$\frac{d^4\Gamma(\bar{B}^0 \to D^{*+}(\to D^0\pi^+)\tau^-\bar{\nu}_\tau)}{dq^2 d\cos\theta d\chi d\cos\theta^*} = \frac{9}{8\pi}|N|^2 J(\theta,\theta^*,\chi),$$

where

$$|N|^2 = \frac{G_F^2|V_{cb}|^2|\mathbf{p}_2|q^2v^2}{(2\pi)^3 12 m_1^2}\mathcal{B}(D^* \to D\pi).$$

The three-angle distribution

The full angular distribution $J(\theta, \theta^*, \chi)$ is written as

$$
\begin{aligned}
& J(\theta, \theta^*, \chi) \\
= \quad & J_{1s} \sin^2\theta^* + J_{1c}\cos^2\theta^* + (J_{2s}\sin^2\theta^* + J_{2c}\cos^2\theta^*)\cos 2\theta \\
& + J_3 \sin^2\theta^* \sin^2\theta \cos 2\chi + J_4 \sin 2\theta^* \sin 2\theta \cos\chi \\
& + J_5 \sin 2\theta^* \sin\theta \cos\chi + (J_{6s}\sin^2\theta^* + J_{6c}\cos^2\theta^*)\cos\theta \\
& + J_7 \sin 2\theta^* \sin\theta \sin\chi + J_8 \sin 2\theta^* \sin 2\theta \sin\chi + J_9 \sin^2\theta^* \sin^2\theta \sin 2\chi,
\end{aligned}
$$

where $J_{i(a)}$ ($i = 1, \ldots, 9; a = s, c$) are coefficient functions depending on q^2, the form factors and the NP couplings.
a large set of observables which can help probe NP in the decay. First, by integrating Eq. (26) over all angles one obtains

$$
\frac{d\Gamma(\bar{B}^0 \to D^* \tau^- \bar{\nu}_\tau)}{dq^2} = |N|^2 J_{\rm tot} = |N|^2 (J_L + J_T),
$$

where J_L and J_T are the longitudinal and transverse polarization amplitudes of the D^* meson, given by

$$
J_L = 3J_{1c} - J_{2c}, \qquad J_T = 2(3J_{1s} - J_{2s}).
$$

It is interesting to note that unlike the vector and scalar operators, which tend to increase both ratios, the tensor operator can lead to a decrease of the ratio $R(D^*)$ for $q^2 \gtrsim 8$ GeV^2. Moreover, while the ratio $R(D^*)$ is minimally sensitive to the scalar coupling S_L the ratio $R(D)$ shows maximal sensitivity to S_L. These behaviors can help discriminate between different NP operators.

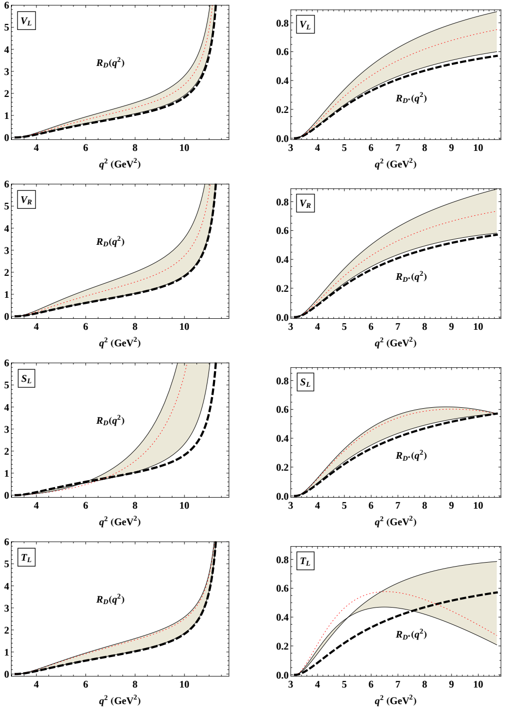

V_L
$R_D(q^2)$
$R_{D^*}(q^2)$
V_R
S_L
T_L
q^2 (GeV^2)

$\cos\theta$ distribution, forward-backward asymmetry & lepton-side convexity

The normalized form of the $\cos\theta$ distribution reads

$$\widetilde{J}(\theta) = \frac{a + b\cos\theta + c\cos^2\theta}{2(a + c/3)}.$$

The linear coefficient $b/2(a + c/3)$ can be projected out by defining a forward-backward asymmetry given by

$$\mathcal{A}_{FB}(q^2) = \frac{(\int_0^1 - \int_{-1}^0) d\cos\theta \, d\Gamma/d\cos\theta}{(\int_0^1 + \int_{-1}^0) d\cos\theta \, d\Gamma/d\cos\theta} = \frac{b}{2(a + c/3)} = \frac{3}{2}\frac{J_{6c} + 2J_{6s}}{J_{\rm tot}},$$

where $J_{\rm tot} = 3J_{1c} + 6J_{1s} - J_{2c} - 2J_{2s}$.
The quadratic coefficient $c/2(a + c/3)$ is obtained by taking the second derivative of $\widetilde{J}(\theta)$. Accordingly, we define a convexity parameter as follows:

$$C_F^{\tau}(q^2) = \frac{d^2\widetilde{J}(\theta)}{d(\cos\theta)^2} = \frac{c}{a + c/3} = \frac{6(J_{2c} + 2J_{2s})}{J_{\rm tot}}.$$

Forward-backward asymmetry $\mathcal{A}_{FB}(q^2)$

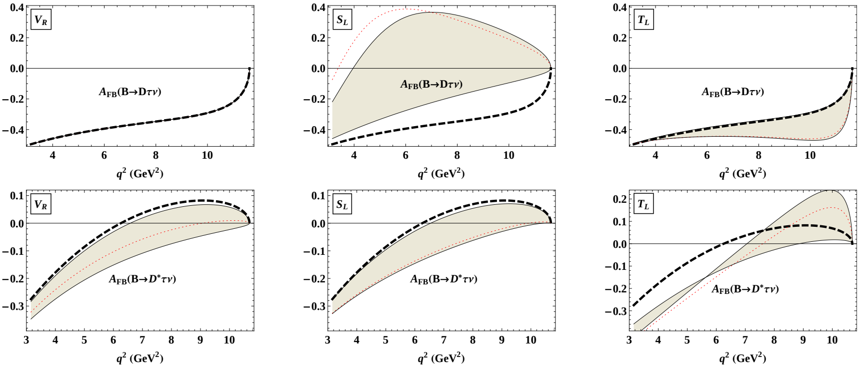

V_L does not effect $\mathcal{A}_{FB}$ in both decays since it stands before the SM operator and drops out in the definition of the observable. For $\bar{B}^0 \to D^*$ transition, $\mathcal{O}_{V_R}$, $\mathcal{O}_{S_L}$, and $\mathcal{O}_{T_L}$ behave mostly similarly: they tend to decrease the FBA and shift the zero-crossing point to greater values than the SM one. However, $\mathcal{O}_{T_L}$ can also increase the asymmetry in the high-q^2 region. For $\bar{B}^0 \to D$, $\mathcal{O}_{V_R}$ does not affect $\mathcal{A}_{FB}$, $\mathcal{O}_{T_L}$ tends to lower $\mathcal{A}_{FB}$, and the scalar operator $\mathcal{O}_{S_L}$ thoroughly changes $\mathcal{A}_{FB}$: it can increase the FBA by up to 200% and implies a zero-crossing point, which is impossible in the SM. This unique effect of $\mathcal{O}_{S_L}$ would clearly distinguish it from the other NP operators.

Lepton-side convexity $C_F^\tau(q^2)$

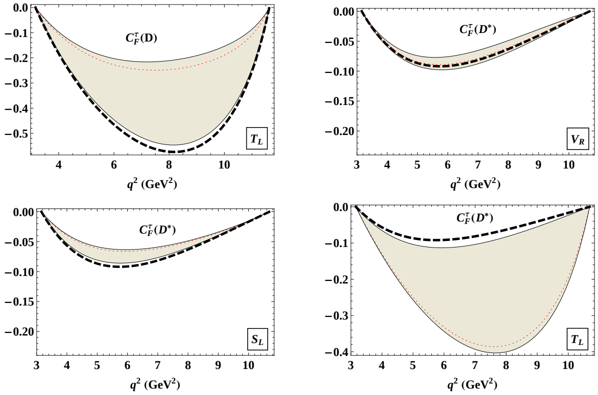

While $C_F^\tau(D)$ is only sensitive to $\mathcal{O}_{T_L}$, $C_F^\tau(D^*)$ is sensitive to $\mathcal{O}_{S_L}$, $\mathcal{O}_{V_R}$, and $\mathcal{O}_{T_L}$. Unlike $\mathcal{O}_{S_L}$, which can only increase $C_F^\tau(D^*)$, the operator $\mathcal{O}_{T_L}$ can only lower the parameter. It is worth mentioning that $C_F^\tau(D)$ and $C_F^\tau(D^*)$ are extremely sensitive to $\mathcal{O}_{T_L}$: it can change $C_F^\tau(D^{(*)})$ by a factor of 4 at $q^2 \approx 7$ GeV^2.

$\cos\theta^*$ distribution and hadron-side convexity parameter

The normalized form of the $\cos\theta^*$ distribution reads $\widetilde{J}(\theta^*) = (a' + c' \cos^2\theta^*)/2(a' + c'/3)$, which can again be characterized by its convexity parameter

$$C_F^h(q^2) = \frac{d^2\widetilde{J}(\theta^*)}{d(\cos\theta^*)^2} = \frac{c'}{a' + c'/3} = \frac{3J_{1c} - J_{2c} - 3J_{1s} + J_{2s}}{J_{\text{tot}}/3}.$$

The $\cos\theta^*$ distribution can be written as

$$\widetilde{J}(\theta^*) = \frac{3}{4}\left(2F_L(q^2)\cos^2\theta^* + F_T(q^2)\sin^2\theta^*\right),$$

where $F_L(q^2)$ and $F_T(q^2)$ are the polarization fractions of the D^* meson and are defined as

$$F_L(q^2) = \frac{J_L}{J_L + J_T}, \qquad F_T(q^2) = \frac{J_T}{J_L + J_T}, \qquad F_L(q^2) + F_T(q^2) = 1.$$

The hadron-side convexity parameter and the polarization fractions of the D^* meson are related by

$$C_F^h(q^2) = \frac{3}{2}\left(2F_L(q^2) - F_T(q^2)\right) = \frac{3}{2}\left(3F_L(q^2) - 1\right).$$

Hadron-side convexity parameter $C_F^h(q^2)$

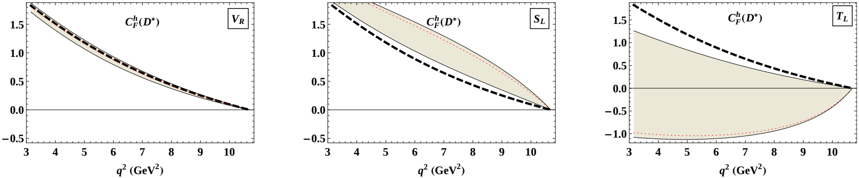

Each NP operator can change $C_F^h(q^2)$ in a unique way:

- $\mathcal{O}_{V_R}$ **almost does nothing to the parameter**
- $\mathcal{O}_{S_L}$ **increases the parameter by about 50% nearly in the whole range of q^2**
- **the tensor operator $\mathcal{O}_{T_L}$ lowers the parameter (by up to 200% at low q^2), and it also allows negative values of $C_F^h(q^2)$, which are impossible in the SM**

Update: First measurement of $F_L^{D^*}$ in the decay $B \to D^*\tau\nu_\tau$ from Belle

Our Analysis: 2016; Belle measurement: 2019

- **Belle Collaboration** A. Abdesselam et al., arXiv:1903.03102
  $F_L^{D^*}(B \to D^*\tau\nu_\tau) = 0.60 \pm 0.08(\mathrm{stat}) \pm 0.04(\mathrm{sys})$
  Agrees with SM within 1.7σ
- **Recent predictions:**
  0.441 ± 0.006 Z.-R. Huang et al., PRD 98, 095018 (2018)
  0.457 ± 0.010 S. Bhattacharya et al., arXiv:1805.08222
- **First prediction (to our knowledge):**
  0.46 M.A. Ivanov, J.G. Körner, C.T. Tran, PRD92 (2015), 114022
- **Crosscheck of Belle:**
  $F_L^{D^*}(B \to D^*\tau\nu_e) = 0.56 \pm 0.02$
  0.54 (the only one) M.A. Ivanov, J.G. Körner, C.T. Tran, PRD92 (2015), 114022

χ distribution and trigonometric moments

The normalized χ distribution reads

$$\widetilde{J}^{(I)}(\chi) = \frac{1}{2\pi}\Big[1 + A_C^{(1)}(q^2)\cos 2\chi + A_T^{(1)}(q^2)\sin 2\chi\Big],$$

where $A_C^{(1)}(q^2) = 4J_3/J_{\rm tot}$ and $A_T^{(1)}(q^2) = 4J_9/J_{\rm tot}$. Besides, one can also define other angular distributions in the angular variable χ as follows

$$J^{(II)}(\chi) = \Big[\int_0^1 - \int_{-1}^0\Big] d\cos\theta^* \int_{-1}^1 d\cos\theta \frac{d^4\Gamma}{dq^2 d\cos\theta d\chi d\cos\theta^*},$$

$$J^{(III)}(\chi) = \Big[\int_0^1 - \int_{-1}^0\Big] d\cos\theta^* \Big[\int_0^1 - \int_{-1}^0\Big] d\cos\theta \frac{d^4\Gamma}{dq^2 d\cos\theta d\chi d\cos\theta^*}.$$

The normalized forms of these distributions read

$$\widetilde{J}^{(II)}(\chi) = \frac{1}{4}\Big[A_C^{(2)}(q^2)\cos\chi + A_T^{(2)}(q^2)\sin\chi\Big],$$

$$\widetilde{J}^{(III)}(\chi) = \frac{2}{3\pi}\Big[A_C^{(3)}(q^2)\cos\chi + A_T^{(3)}(q^2)\sin\chi\Big],$$

where

$$A_C^{(2)}(q^2) = \frac{3J_5}{J_{\rm tot}}, \qquad A_T^{(2)}(q^2) = \frac{3J_7}{J_{\rm tot}}, \qquad A_C^{(3)}(q^2) = \frac{3J_4}{J_{\rm tot}}, \qquad A_T^{(3)}(q^2) = \frac{3J_8}{J_{\rm tot}}.$$

Another method to project the coefficient functions J_i ($i = 3, 4, 5, 7, 8, 9$) out from the full angular decay distribution is to take the appropriate trigonometric moments of the normalized decay distribution $\widetilde{J}(\theta^*, \theta, \chi)$. The trigonometric moments are defined by

$$W_i = \int d\cos\theta d\cos\theta^* d\chi M_i(\theta^*, \theta, \chi)\widetilde{J}(\theta^*, \theta, \chi) \equiv \langle M_i(\theta^*, \theta, \chi)\rangle\,,$$

where $M_i(\theta^*, \theta, \chi)$ defines the trigonometric moment that is being taken. One finds

$$\begin{aligned}
W_T(q^2) &\equiv \langle \cos 2\chi\rangle = \frac{2J_3}{J_{\rm tot}} = \frac{1}{2}A_C^{(1)}(q^2),\\
W_{IT}(q^2) &\equiv \langle \sin 2\chi\rangle = \frac{2J_9}{J_{\rm tot}} = \frac{1}{2}A_T^{(1)}(q^2),\\
W_A(q^2) &\equiv \langle \sin\theta\cos\theta^*\cos\chi\rangle = \frac{3\pi}{8}\frac{J_5}{J_{\rm tot}} = \frac{\pi}{8}A_C^{(2)}(q^2),\\
W_{IA}(q^2) &\equiv \langle \sin\theta\cos\theta^*\sin\chi\rangle = \frac{3\pi}{8}\frac{J_7}{J_{\rm tot}} = \frac{\pi}{8}A_T^{(2)}(q^2),\\
W_I(q^2) &\equiv \langle \cos\theta\cos\theta^*\cos\chi\rangle = \frac{9\pi^2}{128}\frac{J_4}{J_{\rm tot}} = \frac{3\pi^2}{128}A_C^{(3)}(q^2),\\
W_{II}(q^2) &\equiv \langle \cos\theta\cos\theta^*\sin\chi\rangle = \frac{9\pi^2}{128}\frac{J_8}{J_{\rm tot}} = \frac{3\pi^2}{128}A_T^{(3)}(q^2).
\end{aligned}$$

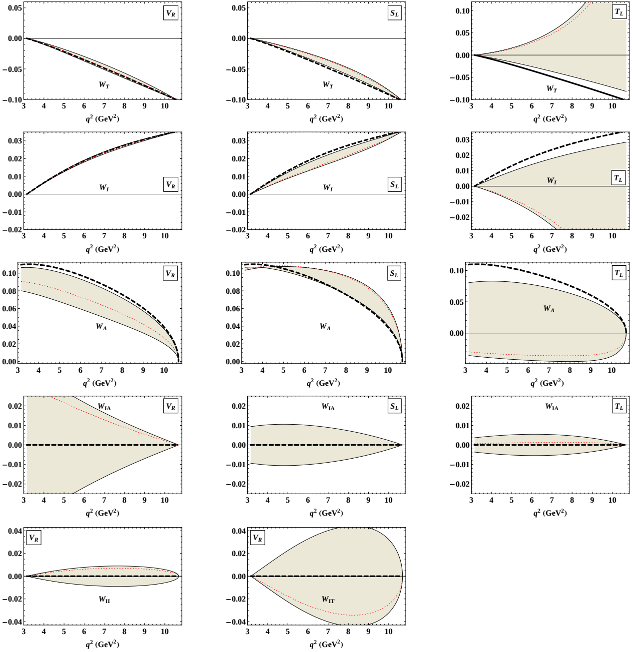

V_R
W_T
q^2 (GeV^2)
S_L
W_T
q^2 (GeV^2)
T_L
W_T
q^2 (GeV^2)
V_R
W_I
q^2 (GeV^2)
S_L
W_I
q^2 (GeV^2)
T_L
W_I
q^2 (GeV^2)
V_R
W_A
q^2 (GeV^2)
S_L
W_A
q^2 (GeV^2)
T_L
W_A
q^2 (GeV^2)
V_R
W_{IA}
q^2 (GeV^2)
S_L
W_{IA}
q^2 (GeV^2)
T_L
W_{IA}
q^2 (GeV^2)
V_R
W_{II}
q^2 (GeV^2)
V_R
W_{IT}
q^2 (GeV^2)

Certain combinations of angular observables where the form factor dependence drops out (at least in most NP scenarios).

$$H_T^{(1)} = \frac{\sqrt{2}J_4}{\sqrt{-J_{2c}(2J_{2s} - J_3)}},$$

which equals to one not only in the SM but also in all NP scenarios except the tensor one. Therefore $H_T^{(1)}(q^2)$ plays a prominent role in confirming the appearance of the tensor operator $\mathcal{O}_{T_L}$ in the decay $\bar{B}^0 \to D^* \tau^- \bar{\nu}_\tau$.

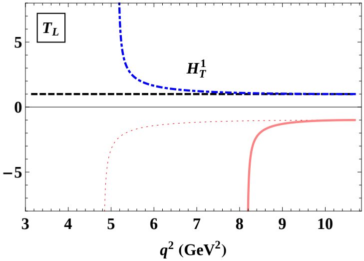

The black dashed line is the SM prediction. The red dotted line, which is almost identical to the SM one, represents the best fit value of T_L. The blue dot-dashed line and the red line are the prediction for $T_L = 0.21i$ and $T_L = 0.18 + 0.27i$, respectively.

Tau polarization in the decays $\bar{B}^0 \to D^{(*)}\tau^-\bar{\nu}_\tau$

- **First measurement by Belle:** [arXiv:1612.00529]

$$P_L^\tau = -0.38 \pm 0.51(\text{stat.})^{+0.21}_{-0.16}(\text{syst.}) \qquad (\text{in } \bar{B}^0 \to D^*\tau^-\bar{\nu}_\tau)$$

- **We define three orthogonal unit vectors as follows:**

$$\vec{e}_L = \frac{\vec{p}_\tau}{|\vec{p}_\tau|}, \qquad \vec{e}_N = \frac{\vec{p}_\tau \times \vec{p}_{D^{(*)}}}{|\vec{p}_\tau \times \vec{p}_{D^{(*)}}|}, \qquad \vec{e}_T = \vec{e}_N \times \vec{e}_L,$$

where $\vec{p}_\tau$ and $\vec{p}_{D^{(*)}}$ - three-momenta of the τ^- and the mesons in the W^- rest frame.

- **Longitudinal (L), normal (N), and transverse (T) polarization four-vectors of the τ^- in the W^- rest frame:**

$$s_L^\mu = \left(\frac{|\vec{p}_\tau|}{m_\tau}, \frac{E_\tau}{m_\tau}\frac{\vec{p}_\tau}{|\vec{p}_\tau|}\right), \qquad s_N^\mu = (0, \vec{e}_N), \qquad s_T^\mu = (0, \vec{e}_T).$$

- **The tau polarization components:**

$$P_i(q^2) = \frac{d\Gamma(s_i^\mu)/dq^2 - d\Gamma(-s_i^\mu)/dq^2}{d\Gamma(s_i^\mu)/dq^2 + d\Gamma(-s_i^\mu)/dq^2}, \qquad i = L, N, T, \qquad q^\mu = p_B^\mu - p_{D^{(*)}}^\mu$$

(Note that $P_N(q^2) = 0$ in the SM.)

Lepton polarization: $\bar{B}^0 \to D^{(*)} e^- \bar{\nu}_e$ vs. $\bar{B}^0 \to D^{(*)} \tau^- \bar{\nu}_\tau$

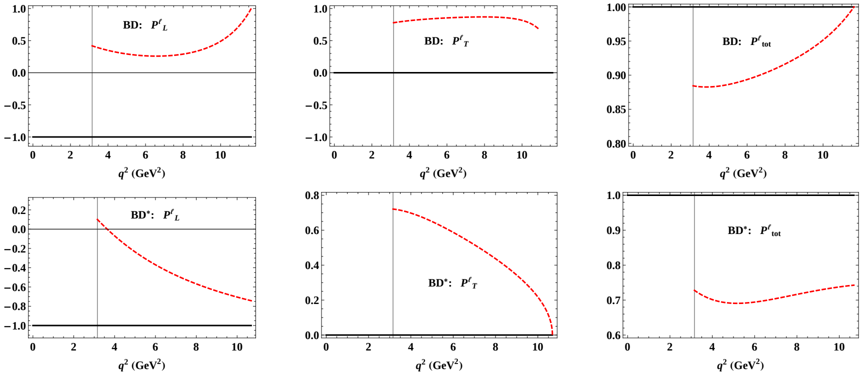

$B \to D\ell^-\bar{\nu}_\ell$: for e^- the curves reflect the chiral limit of a massless lepton in which the lepton is purely left-handed, i.e. one has $P_L^\ell = -1$, $P_T^\ell = 0$, and $|\vec{P}^\ell| = 1$. For τ, P_T^τ is large and positive and dominates the total polarization.
$B \to D^*\ell^-\bar{\nu}_\ell$: When q^2 increases, the longitudinal component becomes larger in magnitude while the transverse polarization becomes smaller. At zero recoil the transverse polarization of the charged lepton P_T^τ tends to zero. The total polarization of the τ has an almost flat behavior with $|\vec{P}^\ell| \sim 0.7$. The overall picture: the polarization is mostly transverse at threshold and turns to longitudinal as q^2 reaches the zero-recoil point.

Result for tau polarization in the SM

P_L-P_T correlation: $\sin\theta_{OD}/\cos\theta_{OD} = P_T/P_L$. Dashed line - $B \to D^*$, solid line - $B \to D$. The arrows show the direction of increasing q^2. The dots on the dashed line stand for $q^2 = 4$, 6, 8, 10 GeV^2. The dots on the solid line - $q^2 = 4$, 8, 10, 11.5 GeV^2

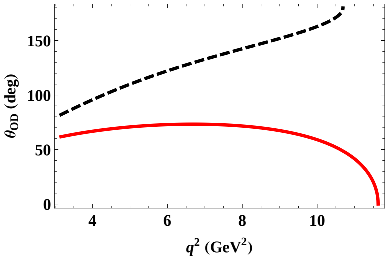

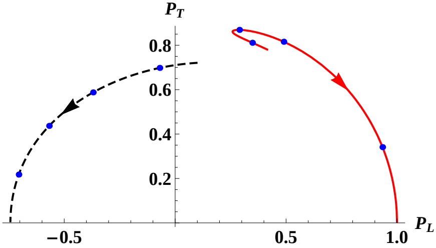

	Our	Other	Ref.
$< P_L^D >$	0.33	0.34 ± 0.03	R. Alonso et al., PRD95 (2017), 093006
		0.325 ± 0.009	M. Tanaka et al.,PRD82 (2010) 034027
$< P_T^D >$	0.84	0.839 ± 0.007	R. Alonso et al., PRD95 (2017), 093006
$< P_L^{D^*} >$	-0.50	-0.497 ± 0.013	M. Tanaka et al., PRD87 (2013), 034028
		$-0.38 \pm 0.51^{+0.21}_{-0.16}$	Belle, PRL 118 (2017), 211801
$< P_T^{D^*} >$	0.46	$\cdots$	$\cdots$

M.A. Ivanov, J.G. Körner, C.T. Tran, PRD92 (2015), 114022

Longitudinal, transverse, and normal polarization of τ^- in $\bar{B}^0 \to D\tau^-\bar{\nu}_\tau$

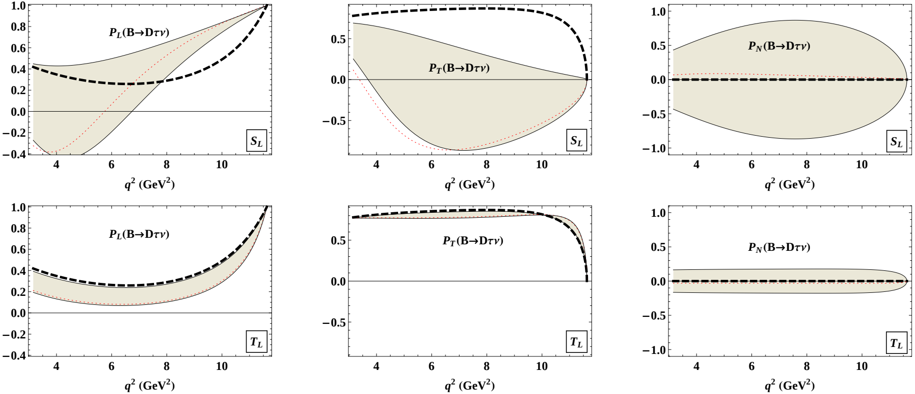

- **Thick black dashed lines: SM prediction**
- **Gray bands include NP effects corresponding to the 2σ allowed regions**
- **Red dotted lines represent the best-fit values of the NP couplings**

Longitudinal, transverse, and normal polarization of τ^- in $\bar{B}^0 \to D^*\tau^-\bar{\nu}_\tau$

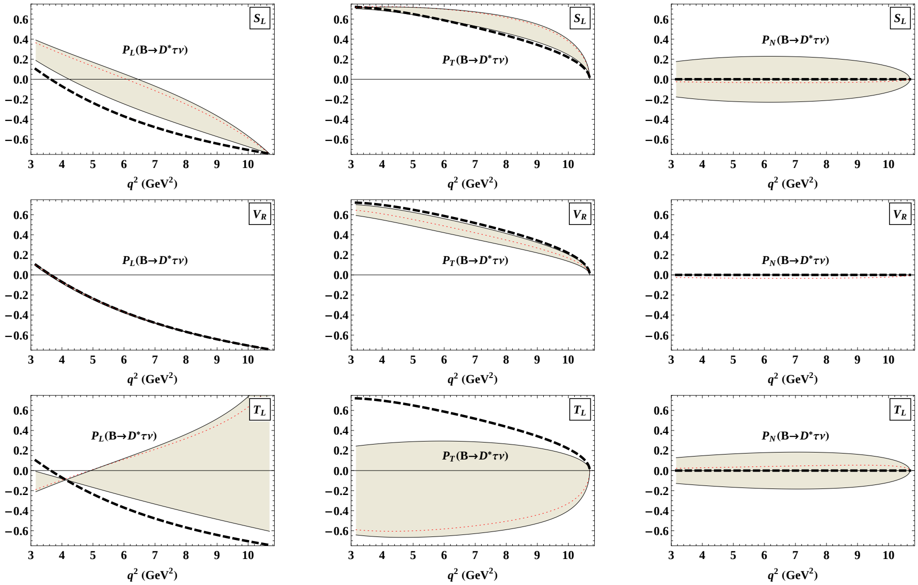

q^2 averages of the polarization components and the total polarization.

One can also calculate the average polarizations over the whole q^2 region. For example, the average longitudinal polarization $\langle P_L^D \rangle$ is calculated by:

$$\langle P_L^D \rangle = \frac{\int dq^2 C(q^2) \left(P_L^D(q^2) \mathcal{H}_{\mathrm{tot}}^D \right)}{\int dq^2 C(q^2) \mathcal{H}_{\mathrm{tot}}^D},$$

where $C(q^2) = |\mathrm{p}_2|(q^2 - m_\tau^2)^2/q^2$ is the q^2-dependent piece of the phase-space factor.

	$\bar{B}^0 \to D$			
	$< P_L^D >$	$< P_T^D >$	$< P_N^D >$	$< \lvert\vec{P}^D\rvert >$
SM (CCQM)	0.33	0.84	0	0.91
S_L	$(0.36, 0.67)$	$(-0.68, 0.33)$	$(-0.76, 0.76)$	$(0.89, 0.96)$
T_L	$(0.13, 0.31)$	$(0.78, 0.83)$	$(-0.17, 0.17)$	$(0.79, 0.90)$
	$\bar{B}^0 \to D^*$			
	$< P_L^{D^*} >$	$< P_T^{D^*} >$	$< P_N^{D^*} >$	$< \lvert\vec{P}^{D^*}\rvert >$
SM (CCQM)	-0.50	0.46	0	0.71
S_L	$(-0.40, -0.14)$	$(0.47, 0.62)$	$(-0.20, 0.20)$	$(0.69, 0.70)$
T_L	$(-0.36, 0.24)$	$(-0.61, 0.26)$	$(-0.17, 0.17)$	$(0.23, 0.69)$
V_R	-0.50	$(0.32, 0.43)$	0	$(0.48, 0.67)$

The predicted intervals for the polarizations in the presence of NP are given in correspondence with the 2σ allowed regions of the NP couplings

Analyzing the polarization of the tau through its decays

As analyzing modes for the τ^- polarization we can consider the four dominant τ^- decay modes

$$\tau^- \to \pi^-\nu_\tau \quad (10.83\%), \qquad \tau^- \to \mu^-\bar{\nu}_\mu\nu_\tau \quad (17.41\%),$$
$$\tau^- \to \rho^-\nu_\tau \quad (25.52\%), \qquad \tau^- \to e^-\bar{\nu}_e\nu_\tau \quad (17.83\%),$$

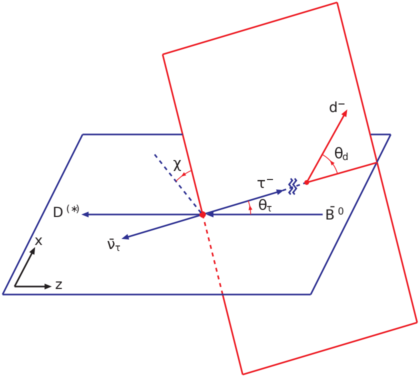

In W rest frame, θ_τ - angle between $\vec{p}_\tau$ and the direction opposite to the direction of the $D^{(*)}$

In τ rest frame, θ_d - angle between d^- and the longitudinal polarization axis, which is chosen to coincide with the direction of the τ in the W rest frame.

χ - azimuthal angle.

- In terms of the angles θ_d and χ, the decay distribution is written as follows:

$$\frac{d\Gamma}{dq^2 d\cos\theta_d d\chi/2\pi} =$$
$$= \quad \mathcal{B}_d \frac{d\Gamma}{dq^2}\frac{1}{2}\big[1 + A_d(P_T(q^2)\sin\theta_d\cos\chi + P_N(q^2)\sin\theta_d\sin\chi + P_L(q^2)\cos\theta_d)\big].$$

  Through an analysis of this decay distribution one can determine the components of the q^2-dependent polarization vector $\vec{P}(q^2) = (P_T(q^2), P_N(q^2), P_L(q^2))$.

- Upon χ integration, one obtains:

$$\frac{d\Gamma}{dq^2 d\cos\theta_d} = \mathcal{B}_d \frac{d\Gamma}{dq^2}\frac{1}{2}\Big(1 + A_d P_L(q^2)\cos\theta_d\Big)$$

  with a polar analyzing power of A_d

- Upon $\cos\theta_d$ integration one has:

$$\frac{d\Gamma}{dq^2 d\chi/2\pi} = \mathcal{B}_d \frac{d\Gamma}{dq^2}\Big(1 + A_d \frac{\pi}{4}(P_T(q^2)\cos\chi + P_N(q^2)\sin\chi)\Big)$$

  with an azimuthal analyzing power of $A_d\pi/4$.

For the decay $\bar{B}^0 \to D^{(*)}\tau^-(\to \rho^-\nu_\tau)\bar{\nu}_\tau$ one has

$$\frac{d\Gamma_\rho}{dq^2 d\cos\theta_\rho d\chi/2\pi} = \mathcal{B}_\rho \frac{d\Gamma}{dq^2}\frac{1}{2}\Big[1+\frac{m_\tau^2-2m_\rho^2}{m_\tau^2+2m_\rho^2}(P_T(q^2)\sin\theta_\rho\cos\chi+P_L(q^2)\cos\theta_\rho)\Big],$$

One looses analyzing power compared to the case $\tau^- \to \pi^-\nu_\tau$:
$(m_\tau^2 - 2m_\rho^2)/(m_\tau^2 + 2m_\rho^2) = 0.4485 < 1$.

One can retain the full analyzing power if one projects out the longitudinal and transverse components of the ρ^-, which can be achieved by an angular analysis of the decay $\rho^- \to \pi^- + \pi^0$ in the rest frame of the ρ^-.

$$\begin{aligned}
\frac{d\Gamma_\rho^L}{dq^2 d\cos\theta_\rho d\chi/2\pi} &= \mathcal{B}_\rho \frac{d\Gamma}{dq^2}\frac{m_\tau^2/2}{m_\tau^2+2m_\rho^2}\Big[1+\big(P_T(q^2)\sin\theta_\rho\cos\chi+P_L(q^2)\cos\theta_\rho\big)\Big] \\
\frac{d\Gamma_\rho^T}{dq^2 d\cos\theta_\rho d\chi/2\pi} &= \mathcal{B}_\rho \frac{d\Gamma}{dq^2}\frac{m_\rho^2}{m_\tau^2+2m_\rho^2}\Big[1-\big(P_T(q^2)\sin\theta_\rho\cos\chi+P_L(q^2)\cos\theta_\rho\big)\Big]
\end{aligned}$$

By separating the two distributions on has regained the full analyzing power of 100% in both cases.

For the leptonic modes $\tau^- \to \ell^- \bar{\nu}_\ell \nu_\tau$ ($\ell = e, \mu$):

$$\frac{d\Gamma_\ell}{dq^2 dx d\cos\theta_\ell d\chi/2\pi} = \frac{d\Gamma}{dq^2}\frac{\Gamma_0}{\Gamma_\tau}\beta x\big[G_1(x)+G_2(x)\big(P_T(q^2)\sin\theta_\ell\cos\chi+P_L(q^2)\cos\theta_\ell\big)\big].$$

Here $x = 2E/m_\tau$, where E–energy of ℓ^- in τ^- rest frame, $\Gamma_0 = G_F^2 m_\tau^5/192\pi^3$, and Γ_τ –total decay width of τ^-.
The coefficient functions:

$$G_1 = x(3-2x) - (4-3x)y^2, \qquad G_2 = \beta x(1 - 2x + 3y^2),$$

where $y = m_\ell/m_\tau$ and $\beta = \sqrt{1 - 4y^2/x^2} = \sqrt{1 - m_\ell^2/E^2} = p/E$.
Polar and azimuthal analyzing power is determined by $G_2(x)/G_1(x)$. By averaging over x ($2y \le x \le 1 + y^2$), one obtains

$$\frac{< \beta x G_2(x) >}{< \beta x G_1(x) >} = -\tfrac{1}{12}(1 + 8y^2 - 32y^3 + \dots).$$

Azimuthal analyzing power:

$$\frac{d\Gamma_\ell}{dq^2 d\chi/2\pi} = \frac{d\Gamma}{dq^2}\frac{\Gamma_0}{\Gamma_\tau}(1+P_T A_\chi \cos\chi), \qquad \text{where} \quad A_\chi = -\frac{\pi}{12}(1+8y^2-32y^3+\dots).$$

For $m_\ell = 0$ one finds $A_\chi = -0.262$ which increases by 3.2% for $m_\ell = m_\mu$.

Implications of new physics in the decays $B_c \to (J/\psi, \eta_c)\tau\nu$

- B_c meson is the lowest bound state of two heavy quarks of different flavors, lying below the $B\bar{D}$ threshold. As a result, while the corresponding $c\bar{c}$ and $b\bar{b}$ quarkonia decay strongly and electromagnetically, the B_c meson decays weakly, making it possible to study weak decays of doubly heavy mesons.
- Weak decays of the B_c meson proceed via the c-quark decays ($\sim 70\%$), the b-quark decays ($\sim 20\%$), and the weak annihilation ($\sim 10\%$).
- First observation of the B_c meson by the CDF Collaboration was made in an analysis of $B_c \to J/\psi\ell\nu$ Phys. Rev. D 58, 112004 (1998).
- LHCb measurement of the ratio of branching fractions

  Phys. Rev. Lett. 120, 121801 (2018)

$$R_{J/\psi} \equiv \frac{\mathcal{B}(B_c \to J/\psi\tau\nu)}{\mathcal{B}(B_c \to J/\psi\mu\nu)} = 0.71 \pm 0.17 \pm 0.18$$

  which lies at about 2σ above the range of existing predictions in the Standard Model (SM).
- At the quark level, the decay $B_c \to J/\psi\ell\nu$ is described by the transition $b \to c\ell\nu$, which is identical to that of the decays $\bar{B}^0 \to D^{(*)}\ell\nu$.

Lecture in this School by A. Issadykov

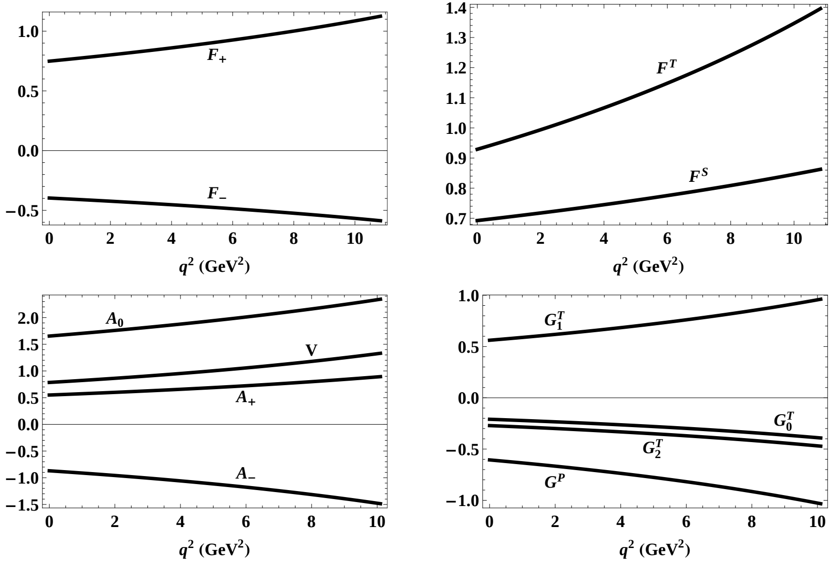

Form factors of the transitions $B_c \to \eta_c$ (upper panels) and $B_c \to J/\psi$ (lower panels).

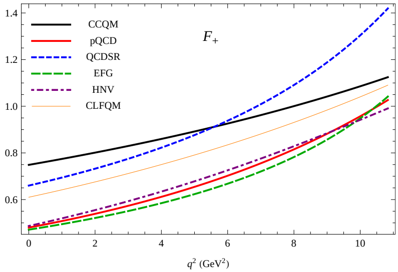

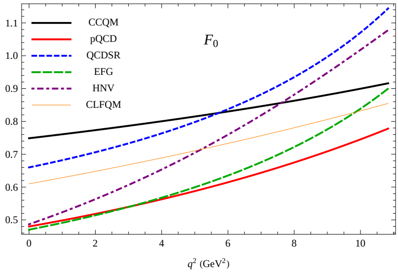

- **perturbative QCD (pQCD)** W. F. Wang et al., Chin. Phys. C 37, 093102 (2013)
- **QCD sum rules (QCDSR)** V. V. Kiselev, arXiv: hep-ph/0211021
- **Ebert-Faustov-Galkin relativistic QM (EFG)** PRD 68, 094020 (2003)
- **Hernandez-Nieves-Velasco (HNV) nonrelativistic QM** PRD 74, 074008 (2006)
- **covariant light-front quark model (CLFQM)** W. Wang et al., PRD 79, 054012 (2009)

Our form factors are very close to those computed in the CLFQM.

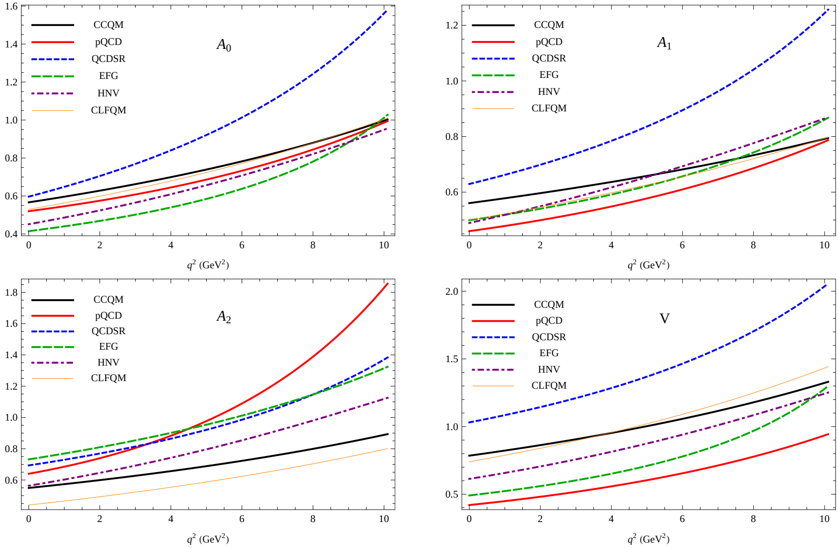

Lattice results for the $B_c \to J/\psi$ FFs by the HPQCD Collab. B. Colquhoun et al., PoS LATTICE 2016, 281 (2016)**: $A_1(0) = 0.49$, $A_1(q^2_{\max}) = 0.79$, and $V(0) = 0.77$**
Our values: $A_1(0) = 0.56$, $A_1(q^2_{\max}) = 0.79$, and $V(0) = 0.78$.

New experimental constraints

- **LHCb measurement**

$$\boxed{R_{J/\psi} = 0.71 \pm 0.17 \pm 0.18}$$

- **R. Alonso, B. Grinstein, J. M. Camalich**

  PRL 118, 081802 (2017)

  "A constraint is obtained by demanding that the rate for $B_c^- \to \tau^- \bar{\nu}$ does not exceed the fraction of the total width that is allowed by the calculation of the lifetime in the SM."

$$\boxed{\mathcal{B}(B_c^- \to \tau^- \bar{\nu}) \lesssim 30\%}$$

- **A. G. Akeroyd, C.-H. Chen**

  PRD 96, 075011 (2017)

  "We show that LEP data taken at the Z peak ($\sqrt{s} \approx 91$ GeV) requires $\mathcal{B}(B_c^- \to \tau^- \bar{\nu}) \lesssim 10\%$ and this constraint is significantly stronger than the recent constraint $\mathcal{B}(B_c^- \to \tau^- \bar{\nu}) \lesssim 30\%$ from considering the lifetime of B_c."

$$\boxed{\mathcal{B}(B_c^- \to \tau^- \bar{\nu}) \lesssim 10\%}$$

We also impose the constraint from the B_c leptonic decay channel. Therefore we need the leptonic branching in the presence of NP operators. The tau mode receives NP contributions from all operators except $\mathcal{O}_{T_L}$:

$$\boxed{\mathcal{B}(B_c \to \tau\nu) = \frac{G_F^2}{8\pi}|V_{cb}|^2 \tau_{B_c} m_{B_c} m_\tau^2 \left(1 - \frac{m_\tau^2}{m_{B_c}^2}\right)^2 f_{B_c}^2 \times \left|1 - g_A + \frac{m_{B_c}}{m_\tau}\frac{f_{B_c}^P}{f_{B_c}} g_P\right|^2}$$

where $g_A \equiv V_R - V_L$, $g_P \equiv S_R - S_L$, τ_{B_c} is the B_c lifetime, f_{B_c} is the leptonic decay constant of B_c, and $f_{B_c}^P$ is a new constant corresponding to the new quark current structure. One has

$$\langle 0|\bar{q}\gamma^\mu\gamma_5 b|B_c(p)\rangle = -f_{B_c} p^\mu, \qquad \langle 0|\bar{q}\gamma_5 b|B_c(p)\rangle = m_{B_c} f_{B_c}^P$$

In the CCQM, we obtain the following values for these constants (all in MeV):

$$f_{B_c} = 489.3, \quad f_{B_c}^P = 645.4.$$

Experimental data: $R_D = 0.407 \pm 0.046$, $R_{D^*} = 0.304 \pm 0.015$ (HFAG-2016), and $R_{J/\psi} = 0.71 \pm 0.25$, as well as the requirement $\mathcal{B}(B_c \to \tau\nu) \leq 10\%$. Within the SM our calculation yields $R_D = 0.267$, $R_{D^*} = 0.238$, and $R_{J/\psi} = 0.24$. We take into account a theoretical error of 10% for our ratios.

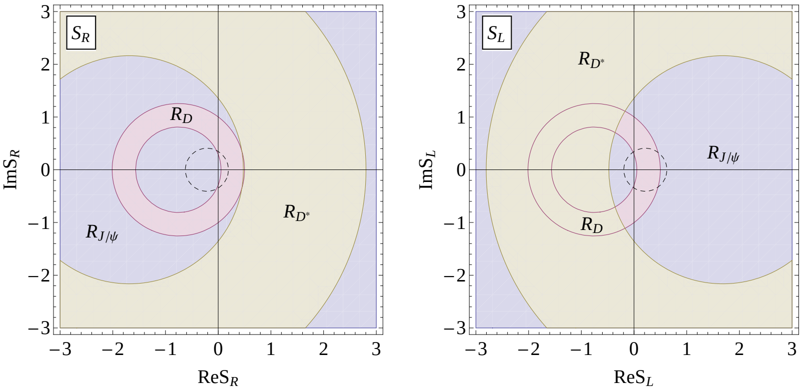

Constraints on the Wilson coefficients S_R and S_L from the measurements of $R_{J/\psi}$, R_D, and R_{D^*} within 2σ, and from the branching fraction $\mathcal{B}(B_c \to \tau\nu)$ (dashed curve).

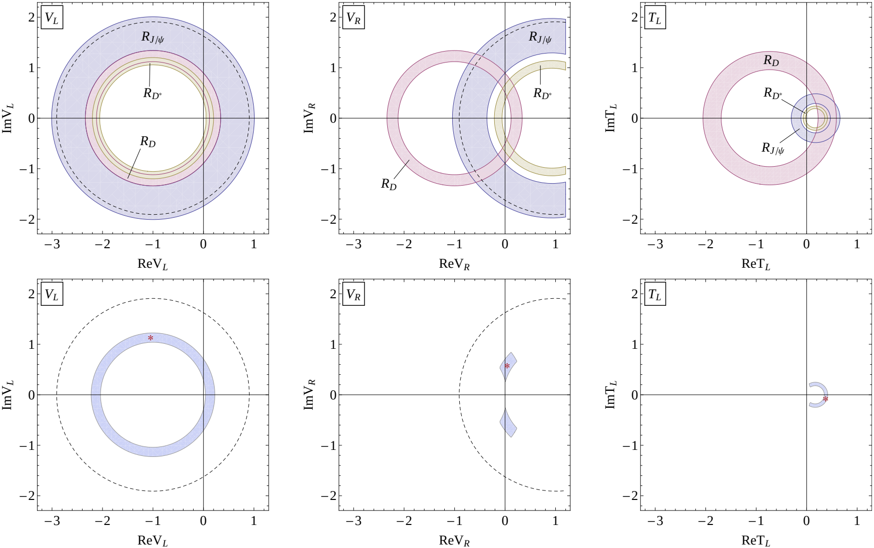

Constraints on the Wilson coefficients V_R, V_L, and T_L from the measurements of $R_{J/\psi}$, R_D, and R_{D^*} within 1σ (upper panels) and 2σ (lower panels), and from the branching fraction $\mathcal{B}(B_c \to \tau\nu)$ (dashed curve).

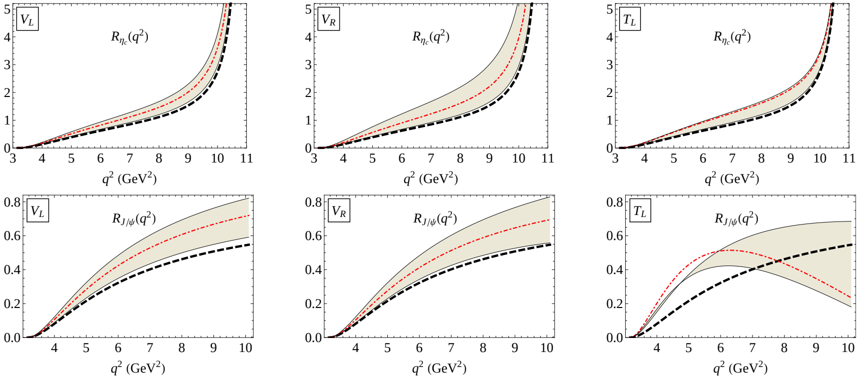

Differential ratios $R_{\eta_c}(q^2)$ (upper panels) and $R_{J/\psi}(q^2)$ (lower panels). The thick black dashed lines are the SM prediction; the gray bands include NP effects corresponding to the 2σ allowed regions; the red dot-dashed lines represent the best-fit values of the NP couplings.

Average values of $R_{J/\psi}$ and R_{η_c} over the whole q^2 region

	$< R_{\eta_c} >$	$< R_{J/\psi} >$
SM	0.26	0.24
V_L	$(0.28, 0.39)$	$(0.26, 0.37)$
V_R	$(0.28, 0.51)$	$(0.26, 0.37)$
T_L	$(0.28, 0.38)$	$(0.24, 0.36)$

- **The row labeled by SM contains our predictions within the SM using our form factors.**
- **The predicted ranges for the ratios in the presence of NP are given in correspondence with the 2σ allowed regions of the NP couplings.**
- **Here, the most visible effect comes from the operator $\mathcal{O}_{V_R}$, which can increase the average ratio $< R_{\eta_c} >$ by a factor of 2.**

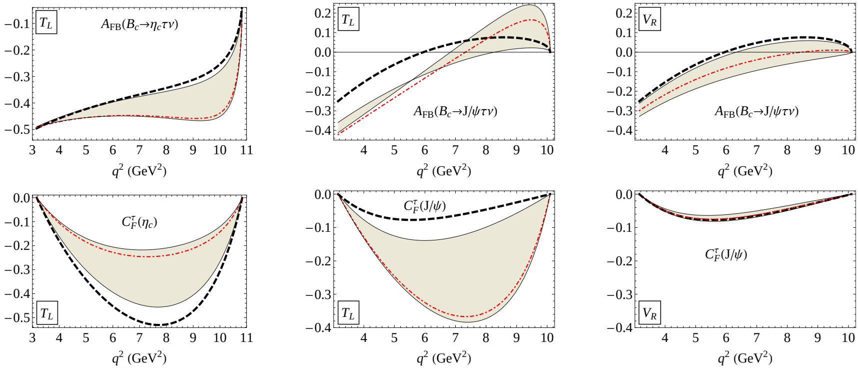

- **For $B_c \to J/\psi$, $\mathcal{O}_{V_R}$ tends to decrease $\mathcal{A}_{FB}$ and shift the zero-crossing point to greater values than the SM one, while $\mathcal{O}_{T_L}$ can enhance $\mathcal{A}_{FB}$ at high q^2.**
- **For $B_c \to \eta_c$, $\mathcal{O}_{V_R}$ does not affect $\mathcal{A}_{FB}$, while $\mathcal{O}_{T_L}$ tends to decrease $\mathcal{A}_{FB}$, especially at high q^2.**
- **Regarding $C_F^\tau(q^2)$: $\mathcal{O}_{V_R}$ has a very small effect on C_F^τ, and only in the case of $B_c \to J/\psi$. In contrast, C_F^τ is extremely sensitive to $\mathcal{O}_{T_L}$. In particular, $\mathcal{O}_{T_L}$ can change $C_F^\tau(J/\psi)$ by a factor of 4 at $q^2 \approx 7.5$ GeV^2. Besides, $\mathcal{O}_{T_L}$ enhances the absolute value of $C_F^\tau(J/\psi)$, but reduces that of $C_F^\tau(\eta_c)$.**

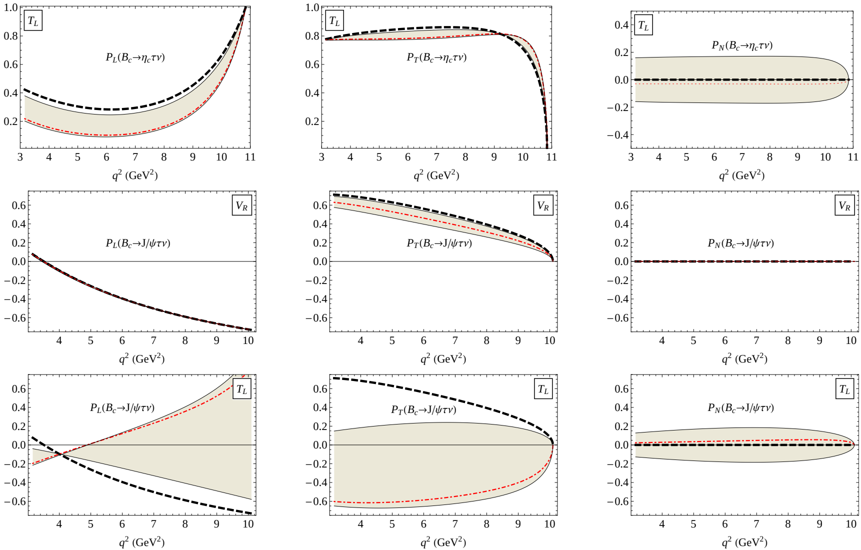

T_L
$P_L(B_c\to\eta_c\tau\nu)$
q^2 (GeV^2)
T_L
$P_T(B_c\to\eta_c\tau\nu)$
q^2 (GeV^2)
T_L
$P_N(B_c\to\eta_c\tau\nu)$
q^2 (GeV^2)
V_R
$P_L(B_c\to J/\psi\tau\nu)$
q^2 (GeV^2)
V_R
$P_T(B_c\to J/\psi\tau\nu)$
q^2 (GeV^2)
V_R
$P_N(B_c\to J/\psi\tau\nu)$
q^2 (GeV^2)
T_L
$P_L(B_c\to J/\psi\tau\nu)$
q^2 (GeV^2)
T_L
$P_T(B_c\to J/\psi\tau\nu)$
q^2 (GeV^2)
T_L
$P_N(B_c\to J/\psi\tau\nu)$
q^2 (GeV^2)

q^2 averages of the forward-backward asymmetry, the convexity parameter, the polarization components

			$B_c \to \eta_c$		
	$< A_{FB} >$	$< C_F^\tau >$	$< P_L >$	$< P_T >$	$< P_N$
SM	-0.36	-0.43	0.36	0.83	0
T_L	$(-0.45, -0.37)$	$(-0.38, -0.19)$	$(0.16, 0.32)$	$(0.78, 0.82)$	$(-0.17, 0$
			$B_c \to J/\psi$		
	$< A_{FB} >$	$< C_F^\tau >$	$< P_L >$	$< P_T >$	$< P_N$
SM	0.03	-0.05	-0.51	0.43	0
V_R	$(-0.09, 0.01)$	$(-0.05, -0.04)$	-0.51	$(0.30, 0.41)$	0
T_L	$(-0.10, 0.01)$	$(-0.31, -0.10)$	$(-0.35, 0.25)$	$(-0.61, 0.21)$	$(-0.17, 0$

Summary

A thorough analysis of possible NP in $\bar{B}^0 \to D^{(*)}\tau^-\bar{\nu}_\tau$ using the FFs obtained from our CCQM. Starting with a general effective Hamiltonian including NP operators, we have derived the full angular distribution and defined a large set of physical observables which helps discriminate between NP scenarios. In particular, we have studied the final tau polarization and its role in probing NP in the decays $\bar{B}^0 \to D^{(*)}\tau^-\bar{\nu}_\tau$. Assuming NP only affects leptons of the third generation and only one NP operator appears at a time, we have gained the allowed regions of NP couplings based on recent measurements at B factories and studied the effects of each operator on the observables. It has turned out that the current experimental data (2016) of $R(D)$ and $R(D^*)$ prefer the operators $\mathcal{O}_{S_L}$ and $\mathcal{O}_{V_{L,R}}$, the operator $\mathcal{O}_{T_L}$ is less favored, and the operator $\mathcal{O}_{S_R}$ is disfavored at 2σ.

Our analysis has been done under the assumption of one-operator dominance. However, the large observable set has revealed unique behaviors of several observables and provided many correlations between them, which allows one to distinguish between NP operators. Our analysis can serve as a map for setting up various strategies to identify the origins of NP. In the future when more precise data will be collected, one can adopt the strategies described in this paper as a useful tool to discover NP in these decays if the deviation from the SM still remains. Finally, we have studied the implications of new physics in the decays $B_c \to (J/\psi, \eta_c)\tau\nu$.

More experimental data now are available. One should redo the analysis to see the new picture.